

Accelerated Randomized Methods for Receiver Design in Extra-Large Scale MIMO Arrays

Victor Croisfelt Rodrigues, Abolfazl Amiri, Taufik Abrão, Elisabeth de Carvalho, Petar Popovski

Abstract—Recent interest has been cast on accelerated versions of the randomized Kaczmarz (RK) algorithm due to the increase in applications that consider sparse linear systems. In particular, considering the context of massive multiple-input-multiple-output (M-MIMO) communication systems, a low complexity naive RK-based receiver has recently been proposed. This method can take advantage of non-stationarities emerging from extra-large M-MIMO systems, but it performs poorly on highly spatially correlated channels. To address this problem, in this paper, we propose a new class of accelerated RK-based receiver designs, where convergence acceleration is based on the residual information. However, we show that the cost of obtaining this knowledge on an iteration basis is not worth it due to the lousy convergence effects caused by system and channel parameters. Inspired by this observation, we further propose a RK-based receiver with sampling without replacement, referred to as RK-RZF. This simple technique is more effective in performing signal detection under reduced complexity. Future works suggest advantage of RK-based receivers to improve current 5G commercial systems and solve the problem of signal detection in other paradigms beyond 5G.

Index Terms—signal detection; massive MIMO; extra-large massive MIMO; randomized Kaczmarz algorithm; residual information.

I. INTRODUCTION

Today's 5G networks are already exploring massive multiple-input multiple-output (M-MIMO) technology to increase data rates and overall system efficiency [1]. Although the fundamentals behind M-MIMO are being deployed, spatial multiplexing is still limited due to the use of compact arrays. With the apparent increase in the number of users that 5G networks must serve, it becomes necessary to i) increase the spatial resolution of antenna arrays to improve performance, and ii) reduce the volume of signal processing running at the base station (BS) to keep it at low cost. One way to increase spatial multiplexing capabilities is to increase the number of antennas and the array size. New challenges emerge for these so-called extra-large M-MIMO (XL-MIMO) systems regarding the second goal: as users become closer to the BS, non-stationarities emerge [2], [3], and the cost of canonical signal detection methods appropriate for scenarios with many users become impractical because of channel matrix inversion and Gramian matrix computation.

V. Croisfelt is with the Electrical Engineering Department, Universidade de São Paulo, Escola Politécnica, São Paulo, Brazil; victorcroisfelt@usp.br.

A. Amiri, E. de Carvalho, and P. Popovski are with the Department of Electronic Systems, Technical Faculty of IT and Design, Aalborg University, Denmark; {aba; edc; petarp}@es.aau.dk.

T. Abrão is with the Electrical Engineering Department, State University of Londrina, PR, Brazil. E-mail: taufik@uel.br

A motivation that arises is the search for efficient and low complexity signal detection methods. Linear receive combining techniques are dominant in M-MIMO systems. State-of-the-art methods include maximum ratio (MR), zero-forcing (ZF), and regularized zero-forcing (RZF) [4]. However, when the number of antennas or of users increases, these methods become excessively expensive.

Many recent publications address the design of efficient and low complexity receivers, a.k.a. relaxed detectors. One of the most common techniques consists of approximating the solution to the minimum-mean squared error (MMSE) criterion applied over signal detection. Three are the key categories to approach this problem [5]: the approximate matrix inversion algorithms [6], the matrix gradient search methods [7], and the iterative solvers of systems of linear equations (SLEs) [8], [9]. The problem with the former is that they quickly approach the complexity of ZF and RZF schemes, and they commonly require channel statistics knowledge [10]. This may not be practical depending on the cost limitation and channel conditions. Although the latter two approaches are the most promising, they can degrade the signal estimates due to channel conditions. In addition, the referred methods can have matrix multiplications in their iterations, making signal processing parallelization difficult to be implemented.

In this paper, we deal with a particular class of iterative methods to solve the MMSE-based signal detection problem which relies on random variants of the Kaczmarz algorithm. The Kaczmarz method is a popular approach for solving very large SLEs. Among the different iterative SLE solvers, a key advantage of Kaczmarz algorithms is the extremely simple and cheap iterations [10], [11]. There are three main characteristics of the Kaczmarz algorithm suitable for solving the problem of interest [10], [12], [13]. First, Kaczmarz iterations only involve scalar/vector-vector operations, making it easy to be *implemented in parallel* [14]. Second, Kaczmarz-based detectors provide more *flexibility*, that is, one can trade-off performance and complexity. Third, under non-stationary channels, Kaczmarz algorithms can benefit from augmented favorable propagation and channel *sparsity* conditions.

A. Related Works

For M-MIMO, the authors of [10] first introduced detection schemes based on the randomized Kaczmarz (RK) algorithm [11]. Their pioneering work focuses on delivering a mathematical background for the application of the RK method in [11] over the MMSE-based signal detection problem. Although

their method is effective considering Rayleigh fading channels, the gain in computational complexity and the effects of spatial correlation were not completely characterized. In [12], we narrowed these gaps by providing more insights on the convergence of a new version of the RK-based detector proposed in [10], but now under spatially correlated and practical estimated channels. Mostly important, We have demonstrated that *RK-based receivers have poor convergence under spatially correlated channels*. Other attempts to use Kaczmarz methods for M-MIMO signal detection are presented in [5], [15]. But these works only consider Rayleigh fading channels and none expected convergence rate has been discussed. In [13], we have introduced the RK-based receiver design [10], [12] in distributed XL-MIMO systems, showing that the method can benefit from non-stationary effects.

The acceleration of convergence in RK methods has gained attention recently due to the increase in applications involving sparse systems and their applicability in machine learning problems. More specifically, we identify important acceleration methods that exploit three types of information related to the SLE being solved: a) iteration residues [16], [17], [18]; b) minimum singular value of the channel coefficient matrix [19], e.g., based on the Nesterov's method [20]; c) sparsity exploitation [21], [22]. All these acceleration approaches share a key feature: although the number of iterations for convergence decreases, the cost per iteration can increase, requiring a rigorous complexity analysis and convergence evaluation.

Importantly, we observe that acceleration techniques based on the iteration residual can take advantage of spatially correlated channels, since the correlation among the residuals is mathematically associated with the correlation of the channel vectors. If the channel vectors of different users are almost orthogonal, the residual information corresponding to the equations of those users will be almost uncorrelated, yielding a reduced number of iterations to attain convergence. However, the problem could remain: the aggregate cost of this reduced number of iterations may be higher. Thus, we propose to verify our observation made above and answer whether this particular class of acceleration methods based on residual information can extend the applicability of RK-based receiver designs when considering more practical M-MIMO and XL-MIMO models and scenarios.

B. Contributions

We propose a new class of receiver designs based on accelerated RK algorithms. In particular, we focus on the acceleration principle that resides in residual information. The new class is applicable for both M-MIMO and XL-MIMO systems. Our ultimate goal is to increase the competitiveness of the RK-based receivers under more practical channel conditions. Precisely, we make the following contributions:

- Full performance-complexity characterization of the proposed RK-based M-MIMO and XL-MIMO detectors under uniform linear array (ULA) and correlated channel model arrangements [4], [23]. Spatially correlated channels consider a compound of the one-ring model [24] with shadowing fluctuations over the array [25]. Non-stationarities are modeled through a diagonal matrix [3].

- A version that adopts sampling without replacement (SwoR) of the hereafter called the naive RK-based receiver (nRK) presented in [10], [12] is considered. This sampling technique helps to combat the biggest disadvantages of nRK without adding much cost.
- A receiver based on the greedy RK (GRK) algorithm [16] is proposed and comprehensively characterized. Compared with nRK, the GRK-based detector has faster convergence and can exploit spatial correlation and non-stationarities due to the using of residual information. But iteration cost is higher.
- Another RK-based receiver based on residual information is proposed accordingly to the randomized sampling Kaczmarz (RSK) method presented in [18]. This method is conceived in an attempt to tackle the problem that the GRK algorithm needs to calculate the residuals of all equations, thus making such procedure unfeasible in certain circumstances.
- In order to standardize the efficiency analysis of the accelerated RK methods in M-MIMO and XL-MIMO detection, a methodology is provided to define the notion of convergence and complexity. Indeed, due to the different iteration costs of the proposed algorithms, we carried out a thorough computational complexity analysis based on counting floating-point operations (flops).

C. Paper Outline

The remainder of this paper is organized as follows. The system model considering spatially correlated Rayleigh fading channels and non-stationarities is presented in Section II. Section III contains the preliminaries necessary to apply accelerated RK algorithms for signal detection. Our proposed class of RK-based receiver designs that emulate the performance of the canonical RZF scheme is presented in Section IV. In Section V, we carried out a complexity analysis and present a convergence definition for the iterative methods. Numerical results evaluating whether the proposed class of accelerated RK-based receivers is practical for M-MIMO and XL-MIMO systems are shown in Section VI. In Section VII, we conclude and present other possible research directions.

D. Notations

Small non-boldface letters are used for constants x , whereas small boldface letters denotes column vectors \mathbf{x} , and capital boldface letters are matrices \mathbf{X} . Calligraphic letters are used for sets of integers \mathcal{X} , and blackboard bold letters mean continuous sets (e.g., \mathbb{C} for the set of complex numbers). Cardinality of a set is given by $|X|$. The n -th element of \mathbf{x} is denoted as x_n , and the m, n -th element of the matrix \mathbf{X} is given by $[X]_{m,n}$. The use of $[X]_{:,n}$ represents the n -th column vector of \mathbf{X} . Vertical and horizontal matrix concatenation are represented as $[X; Y]$ and $[X, Y]$, respectively; the same is used for vectors. We indicate Hermitian transpose by \mathbf{X}^H . Trace and diagonal matrix operators are denoted respectively by $\text{tr}(\cdot)$ and $\text{diag}(\cdot)$. The l_2 -norm of a vector and the Frobenius norm of a matrix are denoted as $\|\mathbf{x}\|_2$ and $\|\mathbf{X}\|_F$, respectively. Gaussian distribution is represented

by $\mathcal{N}(\cdot, \cdot)$, whereas complex-Gaussian distribution is $\mathcal{CN}(\cdot, \cdot)$. Ceil and floor operations are denoted respectively by $\lceil \cdot \rceil$ and $\lfloor \cdot \rfloor$.

II. SYSTEM MODEL

We consider the uplink data phase of a BS equipped with M antennas simultaneously serving a total of K users. For convenience, the group of users is indexed by the set of integers $\mathcal{K} = \{1, 2, \dots, K\}$. We assume a block fading channel model where all of the users' channel vectors $\mathbf{h}_k \in \mathbb{C}^{M \times 1}$ are temporally stationary within a coherence interval [4]. The received baseband signal at the BS $\mathbf{y} \in \mathbb{C}^{M \times 1}$ is then

$$\mathbf{y} = \mathbf{H}\mathbf{x} + \mathbf{n}, \quad (1)$$

where $\mathbf{H} \in \mathbb{C}^{M \times K} = [\mathbf{h}_1, \mathbf{h}_2, \dots, \mathbf{h}_K]$ is the channel matrix, $\mathbf{x} \in \mathbb{C}^{K \times 1}$ is the transmitted signal vector with each entry corresponding to the complex symbol sent by each user, and $\mathbf{n} \in \mathbb{C}^{M \times 1} \sim \mathcal{CN}(\mathbf{0}, \sigma^2 \mathbf{I}_K)$ is the receiver noise vector with noise power equals to σ^2 . Without loss of generality, we assume that symbols are uncorrelated and have zero mean. Since we have considered that users transmit with unit power in (1), the per-user transmit signal-to-noise ratio (SNR) is given by σ^{-2} . Moreover, each user channel vector is distributed as $\mathbf{h}_k \sim \mathcal{CN}(\mathbf{0}, \mathbf{\Theta}_k)$, where $\mathbf{\Theta}_k \in \mathbb{C}^{M \times M}$ is a positive semi-definite spatial correlation matrix.

The loading factor of the system is defined as $LF = K/M$. According to the canonical M-MIMO definition given by [4], we consider under-loaded systems ($LF < 1$), specifically $LF \in [0, 0.5]$. Such interval is the desired operating regime in order to guarantee the benefits brought by M-MIMO of favorable propagation and channel hardening.

A. Channel Model

For a ULA-arranged BS and considering non-line of sight channels, the one-ring model is given by [24]:

$$[\underline{\mathbf{R}}_k]_{m,n} = \frac{1}{2\Delta} \int_{-\Delta}^{\Delta} e^{\pi j(n-m) \sin(\theta_k + \delta)} d\delta, \quad (2)$$

where Δ is the angular spread in radians and θ_k is the k -th user azimuth angle of arrival in radians. The distance between neighbour antennas is half a wavelength.

In this paper, however, we consider a large number of antennas M , justifying the use of iterative methods for signal detection. Having hundreds of antennas operating in sub-6 GHz bands lead to very long ULAs, ranging from a few tens to a hundred of meters. With physically large antenna arrays, two important phenomena observed in practice are not incorporated by the one-ring model. First, wide-sense stationary (WSS) channels do not hold for large antenna arrays [23], [26]. Multipath components do not reach the BS antennas coherently, causing power fluctuations (shadowing) over the array. Second, each user can "see" only portion of the array due to its great size, user proximity, and other blocking effects near BS vicinity. This gives rise to non-stationary channels [2]. The portion of the array viewed by a user is called as the visibility region (VR).

The first effect is modeled by considering independent log-normal large-scale fading (shadowing) variations over the array. Then, the (m, n) -th element of the stationary covariance matrix \mathbf{R}_k is [25]

$$[\mathbf{R}_k]_{m,n} = 10^{(f_m^k + f_n^k)/20} [\underline{\mathbf{R}}_k]_{m,n}, \quad (3)$$

where $f_m^k \sim \mathcal{N}(0, \sigma_{\text{LSF}}^2)$ is the power fluctuation of antenna m and user k . While the general covariance matrix incorporating non-stationary effects can be described as [3]

$$\mathbf{\Theta}_k = \mathbf{D}_k^{\frac{1}{2}} \mathbf{R}_k \mathbf{D}_k^{\frac{1}{2}}. \quad (4)$$

The diagonal matrix $\mathbf{D}_k \in \mathbb{R}^{M \times M}$ models the VR of user k . The particular case of stationary channels occurs when $\mathbf{D}_k = \mathbf{I}_M$, implying $\mathbf{\Theta}_k = \mathbf{R}_k$. For convenience, we assume that, for all users, $\text{tr}(\mathbf{D}_k) = D$, where $D \leq M$ is the number of active antennas for each user.

Fig. 1 represents the overall channel model with the different sources of spatial correlation and non-stationary. Notice that the level of spatial correlation is controlled by the two parameters: Δ and σ_{LSF} . Decreasing Δ and increasing σ_{LSF} , causes overall spatial correction effects to increase, while D establishes which case is being evaluated, stationary ($D = M$) or non-stationary ($D \neq M$) channels.

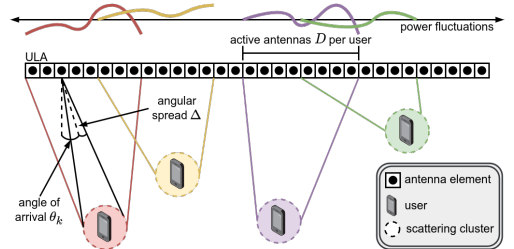


Fig. 1: Illustration of the channel model described by three parameters: angular spread Δ , power fluctuations controlled by σ_{LSF} , and non-stationarities defined by D .

III. PRELIMINARIES

Traditionally, the BS tries to recover the transmitted data signal \mathbf{x} by using a linear receive combining technique over the received signal \mathbf{y} in (1) [4]. The data signal vector detected by the BS is $\hat{\mathbf{x}} = \mathbf{V}^H \mathbf{y}$, where $\mathbf{V} \in \mathbb{C}^{M \times K}$ is the linear receive combining matrix. The latter is a function of the estimated channel matrix $\hat{\mathbf{H}} \in \mathbb{C}^{M \times K}$. Further, we consider that the signal recovery is performed in a centralized manner in both M-MIMO and XL-MIMO systems. Let ξ be the inverse of the per user transmit SNR. For ZF ($\xi = 0$) and RZF ($\xi \neq 0$), a general expression for the estimated signal is defined by:

$$\hat{\mathbf{x}}^{\text{RZF}} = (\mathbf{V}^{\text{RZF}})^H \mathbf{y} = (\hat{\mathbf{H}}^H \hat{\mathbf{H}} + \xi \mathbf{I}_K)^{-1} \hat{\mathbf{H}}^H \mathbf{y}, \quad (5)$$

where $\hat{\mathbf{H}}^H \hat{\mathbf{H}} = \hat{\mathbf{G}} \in \mathbb{C}^{K \times K}$ is the channel Gramian matrix and the term $\hat{\mathbf{G}} + \xi \mathbf{I}_K = \mathbf{R}_{yy} \in \mathbb{C}^{K \times K}$ is the covariance matrix of the received signal \mathbf{y} . Observe that $\hat{\mathbf{G}}$ and \mathbf{R}_{yy} are Hermitian and positive semi-definite matrices.

The problem in directly implementing (5) is mainly the inversion of the $K \times K$ matrix \mathbf{R}_{yy} , remaining true even

for algorithms that exploit the Hermitian property [27], and partly by the Gramian matrix computation $\hat{\mathbf{G}}$. To avoid mostly the matrix inversion, the main idea herein is to pose (5) as the solution of the signal detection problem based on the regularized MMSE criterion. Then, the reformulated problem can be seen as an SLE that can be roughly solved by iterative methods.

A. Signal Detection as an SLE

The classical signal estimate expression in (5) can be viewed as the solution of the following optimization problem:

$$\mathbf{w}^* = \arg \min_{\mathbf{w} \in \mathbb{C}^{K \times 1}} \|\hat{\mathbf{H}}\mathbf{w} - \mathbf{y}\|_2^2 + \xi \|\mathbf{w}\|_2^2, \quad (6)$$

where \mathbf{w}^* is the optimal solution and corresponds to $\hat{\mathbf{x}}^{\text{RZF}}$ [10]. The proof simply follows by taking the derivative of the l_2 -regularized least-squares cost function above and equating it to zero. A compact form of the cost function is $\|\mathbf{B}\mathbf{w} - \mathbf{y}_0\|_2^2$, where $\mathbf{B} \in \mathbb{C}^{(M+K) \times K} = [\hat{\mathbf{H}}; \sqrt{\xi} \mathbf{I}_K]$ and $\mathbf{y}_0 \in \mathbb{C}^{(M+K) \times 1} = [\mathbf{y}; \mathbf{0}]$. Naturally, the solution of this optimization problem can be obtained by solving the over-determined (thin) SLE $\mathbf{B}\mathbf{w} = \mathbf{y}_0$, once $(M+K) > K$.

In M-MIMO and mainly in the XL-MIMO systems, the pair (M, K) can be large enough to make the solution of $\mathbf{B}\mathbf{w} = \mathbf{y}_0$ computationally unfeasible by using direct techniques, that is, variants of Gaussian elimination [28], [29]. This is one of the facts that motivates the use of iterative solvers. Due to the presence of noisy observations, the naive application of these solvers over $\mathbf{B}\mathbf{w} = \mathbf{y}_0$ is not desirable though. In fact, this SLE is inconsistent, meaning that the noisy observations in \mathbf{y} make \mathbf{y}_0 not lie in the range of \mathbf{B} [28]. There is therefore no solution set.¹

Intuitively, it is preferable to solve a consistent SLE if this can be achieved without adding further complexity, which is unbearable [31]. For M-MIMO, the authors of [10] address this problem by applying a transformation over $\mathbf{B}\mathbf{w} = \mathbf{y}_0$.

The transformation yields the following under-determined (fat), consistent SLE:

$$\mathbf{B}^H \mathbf{z} = \mathbf{b} = \hat{\mathbf{H}}^H \mathbf{y}, \quad (7)$$

where $\mathbf{z} \in \mathbb{C}^{(M+K) \times 1} = [\mathbf{u} \in \mathbb{C}^{M \times 1}; \sqrt{\xi} \mathbf{v} \in \mathbb{C}^{K \times 1}]$ and \mathbf{v} corresponds to $\hat{\mathbf{x}}^{\text{RZF}}$ if the system is solved exactly. Notice that each k -th equation in the SLE above can be associated with a user; hence, we can use the terms equation and user interchangeably when discussing the SLE solution. For details on the consistency transformation, we refer to [10], [12], [13].

Remark 1. (Performance Bounds) We recognize \mathbf{b} as the MR estimates $\hat{\mathbf{x}}^{\text{MR}}$ and the price to pay for consistency. Hence, in this paper, the lower bound on performance and complexity are the same found in the MR scheme. Moreover, since the exact solution of (7) is $\hat{\mathbf{x}}^{\text{RZF}}$, RZF scheme is the upper bound on performance and complexity of the iterative methods. One can say that any iterative solver applied over (7) is emulating the RZF scheme.

¹For Kaczmarz methods, an under-relaxation technique is presented in [30] to deal with inconsistency and get the least squares solution of the original SLE. However, this method is difficult to adjust in practice.

Remark 2. (Normal Equations) The authors of [5], [15] designed Kaczmarz-based receivers using the set of normal equations and considering the inverse of \mathbf{V}^{RZF} . The methods discussed here are easily extended to these cases. The costs to obtain these SLEs, however, are higher than the one required to get the SLE in (7). Convergence behavior may also change.

Remark 3. (Limitations and Challenges) Based on the properties of the coefficient matrix $\mathbf{B}^H = [\hat{\mathbf{H}}^H, \sqrt{\xi} \mathbf{I}_K]$, two key reasons make difficult the solution of (7) by iterative methods in general. First, \mathbf{B}^H does not have symmetry properties or is positive definite. Therefore, classical methods that are commonly implemented in linear algebra libraries are not applicable, e.g., generalized minimum residual (GMRES), conjugate gradient square (CGS), and preconditioned conjugate gradient (PCG) [29], [32], [33]. Second, the estimated channel matrix $\hat{\mathbf{H}}$ changes constantly every channel coherence interval due to wireless nature. As a result, the amount of calculations and storage is limited. Techniques that improve convergence naturally become unfeasible in view of these physical restrictions. For example, we can cite practices such as: preconditioning, obtaining the normal equations, as well as the use of other acceleration techniques that needs to be tuned [32], [33].² As we will see, the methods proposed here try to be as simple and effective as possible.

IV. SIGNAL DETECTION BASED ON KACZMARZ RANDOM VARIANT METHODS

In this section, we describe *three random variants* of the Kaczmarz algorithm for solving (7) in a more relaxed way. In particular, one of them is a more practical implementable version of nRK-RZF presented for the first time in [10]. For completeness, the nRK-RZF algorithm has a similar description than the one given in Algorithm 1 below. However, instead of using the SwoR technique in Step 9, nRK samples equations with replacement based on the probability vector given in Step 7.

It is worth mentioning that the RK-based receivers are proposed to solve (7) directly. In other words, the methods are applied for each new channel matrix \mathbf{H} realization. As a practical matter, if the coherence interval is large enough, it is more efficient to calculate the receive combining matrix \mathbf{V} just once and then use it until the end of the coherence interval. Actually, the schemes described here can be generalized in this way by following the lines in [10], [12], [13]. The convergence insights in Section VI-B are also valid for that case, due to the coefficient matrix \mathbf{B}^H be the same.

Intrinsic sparsity from the sub-matrix $\sqrt{\xi} \mathbf{I}_K$ in \mathbf{B}^H of (7) will be clearly exploited when defining the RK-based receivers. Henceforth, the most general case of dense estimated channel matrix $\hat{\mathbf{H}}$ is considered in the mathematical description. Nonetheless, further complexity reduction can be obtained

²For Kaczmarz methods, it is common the use of a relaxation parameter to improve convergence [31]. However, this requires the solution of an optimization problem for adjustment, reducing practicality.

when $\hat{\mathbf{H}}$ is sparse [34].³ For instance, this is theoretically the case of non-stationary channels ($D \neq M$).

A. Randomized Kaczmarz Algorithm

Algorithm 1 summarizes the RK method for solving eq. (7) adopting SwoR in Step 9. We refer to Algorithm 1 as the RK-RZF receiver (see Remark 1). The sub-optimal probabilities $\mathbf{p} \in \mathbb{R}^{K \times 1}$ of selecting each user's equation is given in Step 7.⁴ Each entry of \mathbf{p} can be understood as the power ratios between the powers of each user and the power of the entire system. Both powers are regularized. The more practical sampling technique helps in part to combat the main shortcomings of the old method [10]. But it increases the iteration cost by relating it to the number of equations K .

Algorithm 1 RK for Signal Detection (RK-RZF)

input: $\hat{\mathbf{H}}, \mathbf{y}, M, K, \xi$
output: $\hat{\mathbf{x}}^{\text{RK}}, t^{\text{RK}}$

- 1: $\mathbf{b} = \hat{\mathbf{H}}^H \mathbf{y}$ % $8KM - 2K$ flops
- 2: Store $\{\|\hat{\mathbf{h}}_k\|_2^2 + \xi\}$ % $8KM - K$ flops
- 3: Store $\|\hat{\mathbf{H}}\|_F^2 + K\xi = \sum_{k \in \mathcal{K}} (\|\hat{\mathbf{h}}_k\|_2^2 + \xi)$ % $K - 1$ flops
- 4: $\mathbf{u}^{(0)} \in \mathbb{C}^{M \times 1} = \mathbf{0}$
- 5: $\mathbf{v}^{(0)} \in \mathbb{C}^{K \times 1} = \mathbf{0}$
- 6: $t = 0$
- 7: $\mathbf{p} \in \mathbb{R}^{K \times 1}$ with $p_k = \frac{\|\hat{\mathbf{h}}_k\|_2^2 + \xi}{\|\hat{\mathbf{H}}\|_F^2 + K\xi}$
- 8: **while** termination criterion **is** False **do**
- 9: pick $i^{(t)} \in \mathcal{K}$ based on \mathbf{p} w/ SwoR % K flops
- 10: $r_{i^{(t)}}^{(t)} = b_{i^{(t)}} - \hat{\mathbf{h}}_{i^{(t)}}^H \mathbf{u}^{(t)} - \xi v_{i^{(t)}}$ % $8M + 4$ flops
- 11: $\gamma^{(t)} = r_{i^{(t)}}^{(t)} / (\|\hat{\mathbf{h}}_{i^{(t)}}\|_2^2 + \xi)$ % 2 flops
- 12: $\mathbf{u}^{(t+1)} = \mathbf{u}^{(t)} + \gamma^{(t)} \hat{\mathbf{h}}_{i^{(t)}}$ % $8M$ flops
- 13: $\mathbf{v}^{(t+1)} = \mathbf{v}^{(t)} + \gamma^{(t)} [\mathbf{I}_K]_{:,i^{(t)}}$ % 2 flops
- 14: $t = t + 1$
- 15: **end while**
- 16: $\hat{\mathbf{x}}^{\text{RK}} = \mathbf{v}^{(t)}$
- 17: $t^{\text{RK}} = t$

The main shortcoming of the old nRK-RZF method is related to the probability vector \mathbf{p} in Step 7 of Algorithm 1. The heuristic used to calculate the probability sampling vector is based on power ratios, therefore depending heavily on how the coefficient matrix \mathbf{B}^H is scaled. Hence, when each equation is scaled to have a unit norm, the nRK-RZF method will uniformly draw the equations, $p_k = 1/K$, consequently deteriorating performance [34], [35]. This bad phenomenon is called here as the *curse of uniform normalization*.

For our scenarios of interest, the curse of uniform normalization is related to the adopted BS's power control policy and non-stationary effects. On the one hand, when considering a uniform power control policy, the rows of \mathbf{B}^H have almost

³These gains have two different sources: a) the algorithm can be rewritten to explore a particular sparse structure which reduces, for instance, the number of operations spent in the computation of inner products [22]; b) the overall number of iterations until convergence can be reduced even without rewriting the algorithm, depending on the condition number of the coefficient matrix [11].

⁴Due to natural wireless channel variations, the SLE in (7) is constantly changing. Finding the optimum probability of sampling is very costly and should be computed many times, and, therefore, avoided.

the same l_2 -norms, deteriorating the convergence of the nRK-RZF scheme. On the other hand, when a non-uniform or none power control policy is used, edge-users can suffer from not having their signal estimates recovered reasonably [12], [36]. Truly, very low-power equations are rarely selected by the nRK iteration. Finally, the power scaling also varies for large antenna arrays due to non-stationary channels [3], [26].

With SwoR in Step 9 of Algorithm 1, there are two improvements to the convergence of the old nRK-RZF scheme [10], [12]. First, it avoids the problem of selecting the same equation in sequence [12], improving overall performance. Second, this combats, in part, the curse of uniform normalization, reducing the harmful convergence effect to edge-users. This occurs since users already selected are disregarded until the end of a sweep. A sweep is defined as a cycle of K iterations. In the end of a sweep procedure, the sampling population is the entire set \mathcal{K} .

Algorithm 2 GRK for Signal Detection (GRK-RZF)

input: $\hat{\mathbf{H}}, \mathbf{y}, M, K, \xi$
output: $\hat{\mathbf{x}}^{\text{GRK}}, t^{\text{GRK}}$

- 1: Repeat Steps 1-6 of Algorithm 1 % $16KM - 2K - 1$ flops
- 2: Store $(\|\hat{\mathbf{H}}\|_F^2 + K\xi)^{-1}$ % 1 flop
- 3: **while** termination criterion **is** False **do**
- 4: $\mathbf{r}^{(t)} \in \mathbb{C}^{K \times 1}$ w/ % $8KM - 8$ flops
- $r_k^{(t)} = b_k - \hat{\mathbf{h}}_k^H \mathbf{u}^{(t)} - \xi v_k$
- 5: $\overline{\mathbf{R}}S^{(t)} \in \mathbb{R}^{K \times 1}$ with $\overline{\mathbf{R}}S_k^{(t)} = |r_k^{(t)}|^2$ % $3K$ flops
- 6: $\mathbf{R}SS^{(t)} = \sum_{k \in \mathcal{K}} \overline{\mathbf{R}}S_k^{(t)}$ % $K - 1$ flops
- 7: Compute $\epsilon^{(t)}$ as % $2K + 3$ flops
- $\epsilon^{(t)} = \frac{1}{2} \left(\frac{1}{\mathbf{R}SS^{(t)}} \max_{j \in \mathcal{K}} \left\{ \frac{\overline{\mathbf{R}}S_j^{(t)}}{\|\hat{\mathbf{h}}_j\|_2^2 + \xi} \right\} + \frac{1}{\|\hat{\mathbf{H}}\|_F^2 + K\xi} \right)$
- 8: Get the set of working equations: % $K + 1$ flops
- $\mathcal{U}_t = \left\{ k : \overline{\mathbf{R}}S_k^{(t)} \geq \epsilon^{(t)} \mathbf{R}SS^{(t)} \left(\|\hat{\mathbf{h}}_k\|_2^2 + \xi \right) \right\}$
- 9: $\mathbf{p}^{(t)} \in \mathbb{R}^{K \times 1}$ with % K flops
- $p_k^{(t)} = \begin{cases} \frac{\overline{\mathbf{R}}S_k^{(t)}}{\sum_{j \in \mathcal{U}_t} \overline{\mathbf{R}}S_j^{(t)}}, & \text{if } k \in \mathcal{U}_t \\ 0, & \text{otherwise} \end{cases}$
- 10: pick $i^{(t)} \in \mathcal{U}_t$ based on $\mathbf{p}^{(t)}$
- 11: $\gamma^{(t)} = r_{i^{(t)}}^{(t)} / (\|\hat{\mathbf{h}}_{i^{(t)}}\|_2^2 + \xi)$ % 2 flops
- 12: $\mathbf{u}^{(t+1)} = \mathbf{u}^{(t)} + \gamma^{(t)} \hat{\mathbf{h}}_{i^{(t)}}$ % $8M$ flops
- 13: $\mathbf{v}^{(t+1)} = \mathbf{v}^{(t)} + \gamma^{(t)} [\mathbf{I}_K]_{:,i^{(t)}}$ % 2 flops
- 14: $t = t + 1$
- 15: **end while**
- 16: $\hat{\mathbf{x}}^{\text{GRK}} = \mathbf{v}^{(t)}$
- 17: $t^{\text{GRK}} = t$

B. Greedy Randomized Kaczmarz Algorithm

The GRK algorithm is another random variant of the Kaczmarz algorithm applied to solve SLEs [16]. The key idea

is to annihilate the equations with larger solution residuals as quickly as possible. Essentially, this was heuristically conceived to deal with the curse of uniform normalization and the problem of rare equations. Both present in the nRK algorithm [11], [35]. The application of GRK to solve (7) is presented in Algorithm 2, called as GRK-RZF detection. Additionally, $\tilde{\mathbf{RS}}^{(t)}$ and $\mathbf{RSS}^{(t)}$ stand for the vector of residual squares and the residual sum of squares at iteration t , respectively.

Compared with RK-RZF, the most costly information of GRK-RZF is the residuals of all equations. The elements of the residual vector $\mathbf{r}^{(t)} \in \mathbb{C}^{K \times 1}$ in Step 4 of Algorithm 2 represent such information. One can note that $\mathbf{r}^{(t+1)}$ needs to be entirely recomputed at each new iteration.

Determining which of the equations have larger residuals is the most important step in Algorithm 2. The so-called *working equations* are given by the set \mathcal{U}_t in Step 8 of Algorithm 2. The later is dependent on the intermediate computations of Steps 5-7. The threshold ϵ that represents the average distance can be tuned to improve convergence [31]. We chose not to follow this improvement as we shall see the problem with GRK method is the computation of residuals together with their squared norms.

Probability vector $\mathbf{p}^{(t)} \in \mathbb{R}^{K \times 1}$ in Step 9 of Algorithm 2 is now iteration dependent because of the set \mathcal{U}_t . Despite this, the same heuristic used in Algorithm 1 – Step 7 is also used in Algorithm 2 – Step 9 to compute the sampling probabilities. Thus, the GRK method employs two heuristics: a) the greedy search of larger residuals with the maximum distance rule and b) the sub-optimal sampling probability.

Algorithm 2 can better exploit differences among channel vectors through the residual comparisons carried out in Step 8. Thus, it is expected that GRK-RZF takes more advantage of the channel dissimilarities along the M antennas. These are provided by favorable propagation, spatial correlation, and non-stationarities [2], [4], being those intrinsically related to the correlation among the residuals of different equations. However, due to the increase iteration cost of residual information, it is expected that the Algorithm 1 will perform better than the former for some particular regions of operating values (M, K). As the size of the system grows, the GRK-RZF receiver naturally becomes more attractive than the RK-RZF.

Thinking about increasing the applicability region, one can avoid the use of the residual definition in Step 4 of Algorithm 2 by applying the following recursion [16]:

$$\begin{aligned} \mathbf{r}^{(t+1)} &= \mathbf{b} - \hat{\mathbf{H}}^H \mathbf{u}^{(t+1)} - \xi \mathbf{v}^{(t+1)} \quad (8) \\ &\stackrel{(a)}{=} \mathbf{b} - \hat{\mathbf{H}}^H (\mathbf{u}^{(t)} + \gamma^{(t)} \hat{\mathbf{h}}_{i^{(t)}}) - \xi (\mathbf{v}^{(t)} + \gamma^{(t)} [\mathbf{I}_K]_{:,i^{(t)}}) \\ &= \mathbf{b} - \hat{\mathbf{H}}^H \mathbf{u}^{(t)} - \xi \mathbf{v}^{(t)} - \gamma^{(t)} \hat{\mathbf{H}}^H \hat{\mathbf{h}}_{i^{(t)}} - \gamma^{(t)} \xi [\mathbf{I}_K]_{:,i^{(t)}} \\ &\stackrel{(b)}{=} \mathbf{r}^{(t)} - \gamma^{(t)} (\hat{\mathbf{H}}^H \hat{\mathbf{h}}_{i^{(t)}} + \xi [\mathbf{I}_K]_{:,i^{(t)}}) \\ &\stackrel{(c)}{=} \mathbf{r}^{(t)} - \gamma^{(t)} [\mathbf{R}_{yy}]_{:,i^{(t)}}, \end{aligned}$$

where we have applied: (a) the Kaczmarz iteration relationship, (b) the definition of $\mathbf{r}^{(t)} \in \mathbb{C}^{K \times 1}$, which denotes the residual vector at iteration t , and (c) the definition of the covariance matrix \mathbf{R}_{yy} of the received signal in (5). The recursion is appropriate when the cost of computing \mathbf{R}_{yy} is low compared with the aggregate cost of the iterations.

Henceforth, we denote as rGRK the version of Algorithm 2 that adopts the recursive updating in (8).

C. Randomized Sampling Kaczmarz Algorithm

In an attempt to be more efficient than GRK-RZF in terms of computing time, Algorithm 3 describes the RSK method conceived in [18] to solve the SLE in (7), called as RSK-RZF. The notation $\overrightarrow{\mathbf{RR}}^{(t)}$ means the relative residual vector at iteration t . The main idea of the algorithm is to uniformly select a fixed number of working equations ω in Step 4 in which the residuals are computed and then the equation with the larger residual is chosen to perform the Kaczmarz update. In view of the residual information, it is expected that the RSK-RZF also takes advantage of the differences between the users' channels. But, since RSK-RZF does not explore all residual information in each iteration, it is also expected that its number of iterations until the convergence is higher than the necessary for GRK-RZF. In fact, the number of iterations of the GRK method serves as the lower bound for RSK, and the upper bound is given by the case of $\omega = 1$ in which the equations are drawn uniformly [18].

Algorithm 3 RSK for Signal Detection (RSK-RZF)

input: $\hat{\mathbf{H}}, \mathbf{y}, M, K, \xi, \omega$
output: $\hat{\mathbf{x}}^{\text{RSK}}, t^{\text{RSK}}$

- 1: Repeat Steps 1-6 of Algorithm 1% $16KM - 2K - 1$ flops
- 2: Store $(\|\hat{\mathbf{H}}\|_F^2 + K\xi)^{-1}$ % 1 flop
- 3: **while** termination criterion is False **do**
- 4: Uniformly draw w w/ SwoR \mathcal{U}_t w/ $|\mathcal{U}_t| = \omega$
- 5: $\mathbf{r}^{(t)} \in \mathbb{C}^{K \times 1}$ with % $\omega(8M + 4)$ flops
- 6: $r_j^{(t)} = \begin{cases} b_j - \hat{\mathbf{h}}_j^H \mathbf{u}^{(t)} - \xi v_j, & \text{if } j \in \mathcal{U}_t \\ 0, & \text{otherwise} \end{cases}$
- 7: Compute $\overrightarrow{\mathbf{RR}}^{(t)} \in \mathbb{R}^{K \times 1}$ w/ % 4ω flops
- 8: $\mathbf{RR}_k^{(t)} = |r_k^{(t)}|^2 / (\|\hat{\mathbf{H}}\|_F^2 + K\xi) \forall k \in \mathcal{K}$
- 9: $i^{(t)} = \arg \max_{j \in \mathcal{U}_t} \overrightarrow{\mathbf{RR}}^{(t)}$ % ω flops
- 10: $\gamma^{(t)} = r_{i^{(t)}}^{(t)} / (\|\hat{\mathbf{h}}_{i^{(t)}}\|_2^2 + \xi)$ % 2 flops
- 11: $\mathbf{u}^{(t+1)} = \mathbf{u}^{(t)} + \gamma^{(t)} \hat{\mathbf{h}}_{i^{(t)}}$ % $8M$ flops
- 12: $\mathbf{v}^{(t+1)} = \mathbf{v}^{(t)} + \gamma^{(t)} [\mathbf{I}_K]_{:,i^{(t)}}$ % 2 flops
- 13: $t = t + 1$
- 14: **end while**
- 15: $\hat{\mathbf{x}}^{\text{RSK}} = \mathbf{v}^{(t)}$
- 16: $t^{\text{RSK}} = t$

A problem that arises with Algorithm 3 is how to select ω . The authors of [18] empirically show that a good compromise is to use $\omega = \lceil \log_2 K \rceil$. We carried out experiments varying the parameters of interest and verified that this value is also applicable in our work. Therefore, henceforth, we fixed the value of ω according to this heuristic.

V. COMPLEXITY ANALYSIS AND PRACTICAL CONSIDERATIONS

A. Complexity

Computational complexities of the proposed RK-based receivers are evaluated. When performing the complexity

analysis, we always account for the worst-case. Thus, in Algorithm 1 – Step 7, the SwoR cost is considered to be K flops at most due to the re-normalization of the sampling probability vector. Further, the cardinality of \mathcal{U}_t is always considered to be K , leading to the maximum cost of K flops in Step 9 of Algorithm 2.

Table I summarizes the total number of flops obtained for the relevant detection schemes.⁵ A more detailed description of the flop count is annotated in the algorithms. To take maximal advantage of Kaczmarz iterative structure, some computations that are repeated over the iterations can be computed only once and then be stored for future retrieval. These started with the keyword "Store" in the algorithms. Basically, the steps taken to calculate the RZF scheme were: LAL^H decomposition of \mathbf{R}_{yy} and the solution of the matrix system $\mathbf{L}^H \mathbf{T} = \mathbf{A}^{-1} \mathbf{L}^{-1}$, where \mathbf{A} is diagonal [4], [27].

TABLE I: Detection Time Computational Complexity

Schemes (s)	Time Computational Complexity (C^s) [flops]
MR	$8KM - 2K$
RZF	$4K^2M + 12KM + 5K^3 + 10K^2 - 4K$
nRK-RZK [10]	$16KM - K - 1 + (16M + 8)t^{\text{nRK}}$
RK-RZK	$16KM - 2K - 1 + (K + 16M + 8)t^{\text{RK}}$
GRK-RZF	$16KM - 2K + (8KM + 8M + 7)t^{\text{GRK}}$
rGRK-RZF	$4K^2M + 12KM - K^2 - K + (16K + 8M + 7)t^{\text{rGRK}}$
RSK-RZF	$16KM - 2K + [\omega(8M + 9) + 8M + 4]t^{\text{RSK}}$

[†] $\omega = \lceil \log_2 K \rceil$

B. Implementation Concerns

Previously, the termination or convergence criterion has not been defined precisely. Typically, the use of two termination criteria are employed to break the loop of iterative methods [32]. The first is based on the maximum number of iterations, thus constraining *complexity*. The second uses measures of the *quality* of the run-time approximated solution. Specifically, we opted to use a relative tolerance factor based on the assumption that the solution $\hat{\mathbf{x}}^{\text{RZF}}$ of the SLE (7) is known. Thus, a true error bound can be obtained.

1) *Complexity-Based Termination Criterion*: Let's apply Table I for complexity comparisons of canonical detection schemes with those of the proposed algorithms. By equating the complexities of the proposed receivers with that of the RZF scheme and isolating the number of iterations, we get the maximum number of iterations for each algorithm, listed in Table II. Therefore, when the maximum number of iterations is reached, the complexity of each proposed receiver is the same as that of RZF scheme. Further, if the maximum iteration bounds are reached out, the iterative algorithms terminate independent of solution quality. Note that the bounds are only dependent on the number of BS antennas

⁵**Set of Rules:** 1 complex multiplication corresponds to 4 real multiplications and 2 real additions, or 6 flops, whereas 1 complex addition/subtraction is equivalent to 2 real additions/subtractions or 2 flops. Let $\mathbf{w} \in \mathbb{C}^{N \times 1}$, then $\|\mathbf{w}\|_2^2 = \mathbf{w}^H \mathbf{w}$ costs $8N - 2$ flops, while $\max_{\varphi_n} \varphi$ takes N (lookups) flops in the worst case for $\varphi \in \mathbb{R}^{N \times 1}$. Conjugate transpose and comparisons do not consume relevant computation time. Matrix symmetry is explored whenever possible.

M and the number of users K . An additional termination criterion related to channel could be aggregated since the algorithms' convergence is also influenced by the condition number of the coefficient matrix \mathbf{B}^H in (7), which varies with system and channel parameters [10], [12], [13]. On the other hand, when deploying RK-based receivers, it is easy to calculate the maximum iteration bounds given in the table and control performance-complexity trade-off through it.

TABLE II: Maximum Number of Iterations

Schemes (s)	Max. Iterations (t_{\max}^s)
nRK-RZK [10]	$\left\lceil \frac{\text{num} - K + 1}{16M + 8} \right\rceil$
RK-RZK	$\left\lceil \frac{\text{num} + 1}{K + 16M + 8} \right\rceil$
GRK-RZF	$\left\lceil \frac{\text{num}}{8KM + 8M + 7} \right\rceil$
rGRK-RZF	$\left\lceil \frac{5K^3 + 11K^2 - 3K}{16K + 8M + 7} \right\rceil$
RSK-RZF	$\left\lceil \frac{\text{num}}{\omega(8M + 9) + 8M + 4} \right\rceil$

[†] $\omega = \lceil \log_2 K \rceil$

^{*} $\text{num} = 4K^2M - 4KM + 5K^3 + 10K^2 - 2K$

2) *Quality Termination Criterion*: Assuming that $\hat{\mathbf{x}}^{\text{RZF}}$ is known, the quality tolerance criterion based on the *relative solution error* (RSE) can be defined by the condition [16]:

$$\text{RSE}^i = \frac{\|\hat{\mathbf{x}}^i - \hat{\mathbf{x}}^{\text{RZF}}\|_2^2}{\|\hat{\mathbf{x}}^{\text{RZF}}\|_2^2} \leq \text{rtol}, \quad (9)$$

where i indexes the different proposed algorithms and rtol is the theoretical relative tolerance, a positive constant, typically in the range $\text{rtol} \in [10^{-2}, 10^{-6}]$. The criterion in (9) must be true for the algorithm to finish. An interesting point to observe is that rtol also strongly controls the performance-complexity trade-off.

VI. NUMERICAL RESULTS

In this section, we empirically demonstrate whether the proposed class of accelerated RK-based receivers perform better than the nRK-RZF method considered in previous works [10], [12], [13]. To evaluate communication performance, we use the bit-error-rate (BER) metric. For all simulations, we assume that the transmit signal vector \mathbf{x} is drawn from a 16-QAM constellation. The constellation is normalized to have unit average power and the sequential symbol order is considered. Median number of iterations or, simply, iterations is denoted by IT [iterations] or [iters.]. This value is obtained from the simulations and plugged into Table I to compute the complexities of each proposed algorithm. Moreover, we disregard long-term fading coefficients (pathloss), since in this particular scenario the performance of the RK-based receivers tends to worsen due to the low variability on the scale of the l_2 -norms of the estimated channel vectors $\{\|\hat{\mathbf{h}}_k\|_2\}$. Finally, for fairness reasons, we ignore any further gains that Kaczmarz algorithms may have due to parallel computing over inverse matrix parallel computation.

A. Channel Generation

The steps required to obtain channel estimates under spatial non-stationary effects include: a) generation of channel matrix estimates and b) emulation of the spatial non-stationarities in XL-MIMO scenarios. Estimated channel matrix is given by the following general model:

$$\hat{\mathbf{H}} = \sqrt{1 - \gamma^2} \cdot \mathbf{H} + \gamma \cdot \mathbf{N} = [\hat{\mathbf{h}}_1, \hat{\mathbf{h}}_2, \dots, \hat{\mathbf{h}}_K], \quad (10)$$

where $\gamma \in [0, 1]$ is the estimation quality parameter and $\mathbf{N} \in \mathbb{C}^{M \times K}$ is the noise matrix with i.i.d. entries $[N]_{m,k} \sim \mathcal{CN}(0, 1)$ [10]. Perfect ($\gamma = 0$) and imperfect ($\gamma > 0$) channel estimation cases are considered in simulation results.

In order to emulate non-stationarities, we consider, for simplicity, the case where the diagonal matrix \mathbf{D}_k is an indicator matrix. In this case, the number of active antennas D is a natural number different from zero and upper bounded by M . When $D = M$, we have the stationary case. To generate a collection of K diagonal matrices \mathbf{D}_k , we adopt the procedure described in [3]. Moreover, we embrace the normalization that ensures same norm for stationary and non-stationary channels [3].

B. Convergence Behavior

In this part, the convergence of the proposed algorithms is compared, hence, we disregard the maximum number of iterations bounds in Table II while set the maximum iteration to 200,000 iterations for all algorithms, just to ensure a reasonable simulation time. The relative tolerance is fixed as $rtol = 10^{-6}$, attaining the notion of full convergence. This is sufficient to ensure that all RK-based receivers have almost the same performance as that provided by the RZF scheme. Moreover, recall that the median iterations for GRK-RZF and rGRK-RZF are the same.

Fig. 2 depicts the most important convergence breakthroughs in terms of median iterations. When channel parameters are analyzed, each parameter is treated independently. For example, when varying the angular spread Δ , we set $\sigma_{LSF} = 0$ and $D = M$.

As the loading factor LF increases, the gaps between RK-based receivers that do not use residual information and those which do increase. Thus, accelerated RK methods based on residual information are more suitable for large LF values. Conversely, when increasing the angular spread Δ and the number of active antennas D , the same gaps tend to shrink, as expected. Hence, the convergence of accelerated RK methods based on residual information are faster along all the angular spread range and active number of antennas, but specially advantageous under highly spatially correlated channels ($\downarrow \Delta$) and increased level of non-stationary ($\downarrow D$). As a result, there is a direct consequence of the intrinsic mathematical relationship between correlation among channel vectors and the correlation among the residuals of the equations. Finally, shadowing fluctuations controlled by σ_{LSF} do not seem to interfere with the convergence performance of the methods. One reason for this is that we are disregarding pathloss variations; thus power fluctuations only affect the variability of the number of iterations needed to attain

convergence. Importantly, an advantage of accelerated GRK-RZF and RSK-RZF algorithms, is that their distributions of the number of iterations are flatter, implying lower variability.

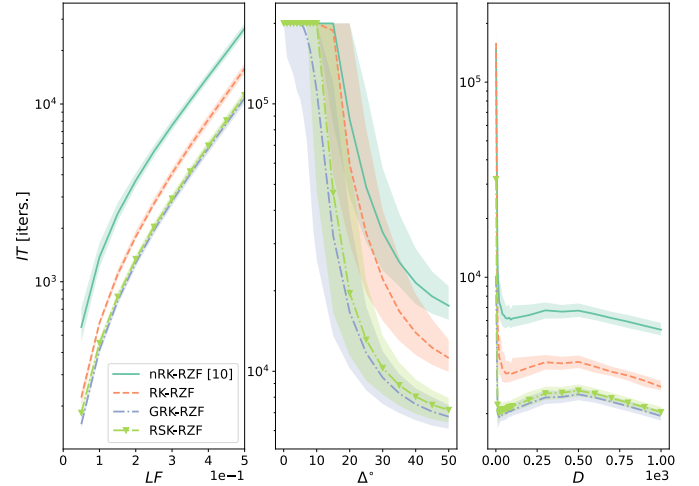


Fig. 2: Median number of iterations IT of the proposed algorithms. *Left*: loading factor LF varying under Rayleigh fading and stationary channels. *Middle*: angular spread Δ varying with $\sigma_{LSF} = 0$, $LF = 0.25$, and under stationary channel. *Right*: number of active antennas D varying with $LF = 0.25$ and under Rayleigh fading channels. Shaded regions are the 5th and 95th percentiles, measured over 1000 trials. Other parameters are fixed as follows: $M = 1000$ antennas, SNR = 5 dB, and perfect estimation quality $\gamma = 0$.

C. Performance-Complexity Trade-Off

We now evaluate the efficiency in terms of performance-complexity trade-off of the proposed RK-based receivers in comparison with the classical MR and RZF schemes. We run the iterative algorithms until they reach their respective maximum number of iterations bounds given in Table I. However, we have disregarded the quality termination criterion $rtol$; thus, the performance of the proposed receiver algorithms may vary and, in fact, be adjusted to practical performance upper bounds. In other words, from those points on, if we want to improve the performance of the algorithms and reach the theoretical upper limit of performance given by the RZF scheme, we must pay with greater complexity than necessary to obtain RZF signal estimates. *Therefore, the most competitive RK-based receiver design approach is that most closely matches the performance of the RZF scheme when considering variations in system and channel parameters.*

The effectiveness of the relevant receiver designs are demonstrated for both scenarios of interest: M-MIMO (Fig. 3) and XL-MIMO (Fig. 4) systems.

Fig. 3 shows the average performance of the analyzed receiver designs for the M-MIMO case. The results presented in the figures reveal that the general class of all RK-based receivers performs considerably worse in terms of RZF performance for M-MIMO systems with spatially correlated channels. This is inline with what is expected from previous works [12], [13]. One of the reasons for this low

efficiency is that the SLE in (7) is not big enough to justify the use of iterative methods. However, note that some of the performances achieved by RK-based receivers are still reasonable, since we are disregarding channel coding. We can thus still benefit from the other practical advantages brought by the use of the Kaczmarz algorithm. The most important observation we can get from these figures is that our proposed RK-RZF, which adopts SwoR, outperforms all the other methods and is enough to improve the performance of the old nRK-RZF in M-MIMO systems. Furthermore, this means that methods based on residual information are still expensive for the size of the system considered.

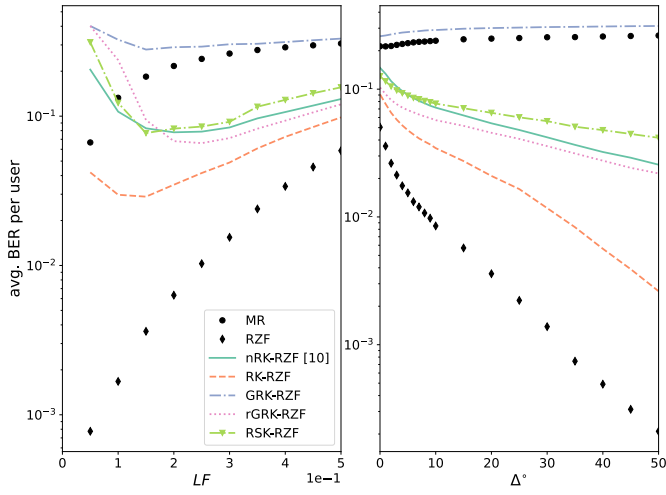


Fig. 3: Comparison of performance for M-MIMO scenario. *Left:* LF is varying with $\Delta = 10^\circ$. *Right:* Δ is varying and $LF = 0.25$. Fixed parameters are: $M = 100$ antennas, $SNR = 5$ dB, power fluctuations of $\sigma_{LSF} = 2$, stationary channels $D = M$, and estimation quality of $\gamma = 0.1$.

On the other hand, the simulation results depicted in Fig. 4 reveal significant performance improvements of the RK-based receivers operating under XL-MIMO configuration when compared with the theoretical limit given by the RZF and MR schemes. This is so because of the size of the problem in (7) and the benefit brought by non-stationarities. In some particular regions, mainly under the case of high user interference and in channels with high spatial correlation and high level of non-stationarities, rGRK-RZF performs marginally better than the most competitive scheme, the RK-RZF. But, in general, the latter outperforms the other proposed schemes. Consequently, at least for the size of the systems considered, RK-RZF is sufficient to partially reduce the shortcomings of nRK-RZF without adding much cost. Thus, although the class of accelerated RK-based receivers that use residual information has a smaller number of iterations (see Fig. 2), this advantage does not justify in general the high cost of obtaining such information per iteration. Moreover, note that in both evaluated BS antenna scenarios the RSK-RZF receiver performs better than GRK-RZF, as expected; however, it turns out that rGRK-RZF is more effective than the former most of the time.

VII. CONCLUSIONS

In an attempt to increase the practicality of RK methods in M-MIMO and XL-MIMO system scenarios, we have proposed a new class of accelerated RK-based receiver designs based on residual information. Besides, we have considered the RK method with SwoR, referred to as RK-RZF receiver, in order to combat the previous flaws of the RK-based receivers presented in the literature without adding much computational cost. We have numerically confirmed our conjecture that the use of residual information further increases the convergence speed of RK-based receivers. This happens mainly in scenarios with many users operating under high spatial correlation channels and high level of non-stationary effects. Although accelerated RK methods need fewer iterations to converge, the cost of obtaining residual information is quite high. This reduces the effectiveness of these particular accelerated algorithms and we thus observe that the RK-RZF scheme is the most competitive for more practical channel assumptions. It may be that the use of residual information can still be effective when associated with other acceleration techniques.

Future research may take advantage of the methodology presented here for evaluation of other acceleration techniques. In addition, distributed ways for solving SLEs with RK-based methods are well-known in wireless sensor network research (e.g., [37]). Our vision is that these distributed approaches can be adapted for application in cell-free M-MIMO and distributed XL-MIMO systems, seeing antenna subarrays and unique antennas as the wireless nodes. Therefore, we encourage the use of the RK-RZF detector to design these distributed receivers in paradigms beyond 5G.

ACKNOWLEDGMENT

The authors are supported in part by the Coordenação de Aperfeiçoamento de Pessoal de Nível Superior (CAPES) – Brazil - Finance Code 001, in part by the National Council for Scientific and Technological Development (CNPq) of Brazil under Grant 310681/2019-7, Fundação Araucária under Grant PBA-3673/2016, and in part by São Paulo University – São Paulo Government (USP). Victor Croisfelt is supported by Universidade de São Paulo with the Coordenação de Aperfeiçoamento de Pessoal de Nível Superior (CAPES) – Brazil under Grant 88887.461434/2019-00.

REFERENCES

- [1] E. Björnson, L. Sanguinetti, H. Wymeersch, J. Hoydis, and T. L. Marzetta, "Massive MIMO is a reality—What is next?: Five promising research directions for antenna arrays," *Digital Signal Processing*, vol. 94, pp. 3 – 20, 2019, special Issue on Source Localization in Massive MIMO.
- [2] E. D. Carvalho, A. Ali, A. Amiri, M. Angjelichinoski, and R. W. Heath, "Non-Stationarities in Extra-Large-Scale Massive MIMO," *IEEE Wireless Communications*, vol. 27, no. 4, pp. 74–80, aug 2020.
- [3] A. Ali, E. D. Carvalho, and R. W. Heath, "Linear Receivers in Non-Stationary Massive MIMO Channels With Visibility Regions," *IEEE Wireless Communications Letters*, vol. 8, no. 3, pp. 885–888, jun 2019.
- [4] E. Björnson, J. Hoydis, and L. Sanguinetti, "Massive MIMO Networks: Spectral, Energy, and Hardware Efficiency," *Foundations and Trends® in Signal Processing*, vol. 11, no. 3-4, pp. 154–655, 2017.

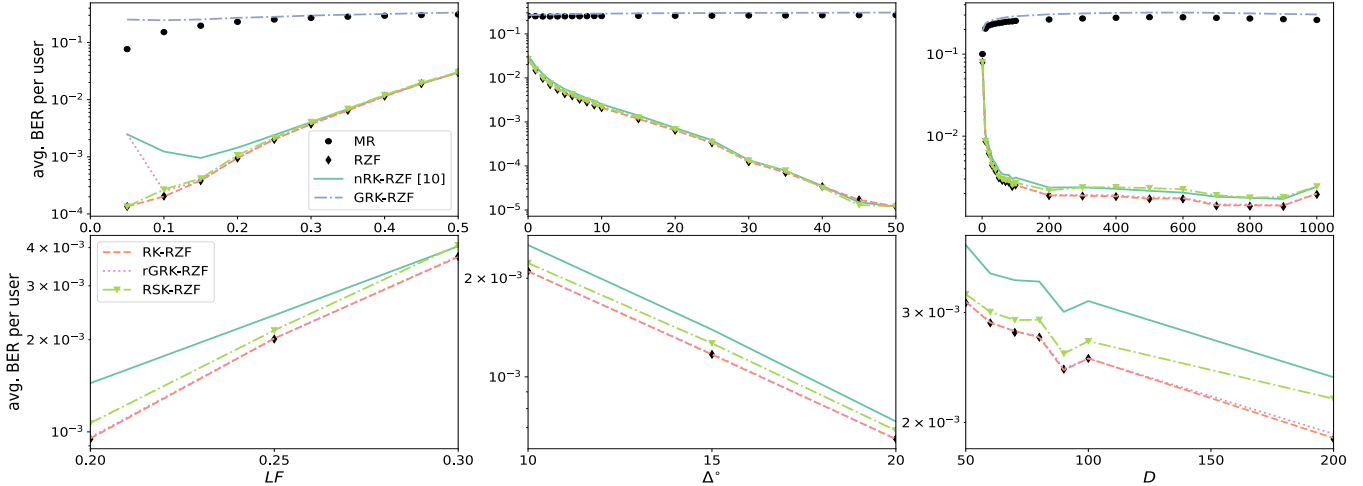


Fig. 4: Comparison of performance for XL-MIMO scenario. *Left:* LF is varying with $\Delta = 10^\circ$, $D = 100$. *Middle:* Δ is varying and $LF = 0.25$, $D = 100$. *Right:* D is varying and $LF = 0.25$, $\Delta = 10^\circ$. Fixed parameters are: $M = 1000$ antennas, SNR = 5 dB, power fluctuations of $\sigma_{LSF} = 2$, and estimation quality of $\gamma = 0.1$.

- [5] H. Wu, B. Shen, S. Zhao, and P. Gong, "Low-Complexity Soft-Output Signal Detection Based on Improved Kaczmarz Iteration Algorithm for Uplink Massive MIMO System," *Sensors*, vol. 20, no. 6, p. 1564, mar 2020.
- [6] A. Muller, A. Kammoun, E. Bjornson, and M. Debbah, "Efficient linear precoding for massive MIMO systems using truncated polynomial expansion," in *2014 IEEE 8th Sensor Array and Multichannel Signal Processing Workshop (SAM)*. IEEE, jun 2014, pp. 273–276.
- [7] B. Yin, M. Wu, J. R. Cavallaro, and C. Studer, "Conjugate gradient-based soft-output detection and precoding in massive MIMO systems," in *2014 IEEE Global Communications Conference*. IEEE, dec 2014, pp. 3696–3701.
- [8] X. Gao, L. Dai, C. Yuen, and Y. Zhang, "Low-Complexity MMSE Signal Detection Based on Richardson Method for Large-Scale MIMO Systems," in *2014 IEEE 80th Vehicular Technology Conference (VTC2014-Fall)*. IEEE, sep 2014, pp. 1–5.
- [9] L. Dai, X. Gao, X. Su, S. Han, C.-L. I, and Z. Wang, "Low-Complexity Soft-Output Signal Detection Based on Gauss-Seidel Method for Uplink Multiuser Large-Scale MIMO Systems," *IEEE Transactions on Vehicular Technology*, vol. 64, no. 10, pp. 4839–4845, oct 2015.
- [10] M. N. Boroujerdi, S. Haghaghshoar, and G. Caire, "Low-Complexity Statistically Robust Precoder/Detector Computation for Massive MIMO Systems," *IEEE Transactions on Wireless Communications*, vol. PP, no. c, p. 1, 2018.
- [11] T. Strohmer and R. Vershynin, "A Randomized Kaczmarz Algorithm with Exponential Convergence," *Journal of Fourier Analysis and Applications*, vol. 15, no. 2, pp. 262–278, apr 2009.
- [12] V. C. Rodrigues, J. C. Marinello Filho, and T. Abrão, "Randomized Kaczmarz algorithm for massive MIMO systems with channel estimation and spatial correlation," *International Journal of Communication Systems*, p. e4158, sep 2019.
- [13] V. C. Rodrigues, A. Amiri, T. Abrão, E. de Carvalho, and P. Popovski, "Low-Complexity Distributed XL-MIMO for Multiuser Detection," in *2020 IEEE International Conference on Communications Workshops (ICC Workshops)*. IEEE, jun 2020, pp. 1–6.
- [14] J. D. Moorman, T. K. Tu, D. Molitor, and D. Needell, "Randomized Kaczmarz with averaging," *BIT Numerical Mathematics*, pp. 1–19, 2020.
- [15] Y. Lee, "Hybrid Kaczmarz and coordinate-descent iterations for signal detection in massive MIMO systems," *Electronics Letters*, vol. 55, no. 11, pp. 665–667, 2019.
- [16] Z. Z. Bai and W. T. Wu, "On Greedy Randomized Kaczmarz Method for Solving Large Sparse Linear Systems," *SIAM Journal on Scientific Computing*, vol. 40, no. 1, pp. A592–A606, 2018.
- [17] ———, "On relaxed greedy randomized Kaczmarz methods for solving large sparse linear systems," *Applied Mathematics Letters*, vol. 83, pp. 21–26, 2018.
- [18] M.-L. Sun, C.-Q. Gu, and P.-F. Tang, "On Randomized Sampling Kaczmarz Method with Application in Compressed Sensing," *Mathematical Problems in Engineering*, vol. 2020, pp. 1–11, mar 2020.
- [19] J. Liu and S. J. Wright, "An Accelerated Randomized Kaczmarz Algorithm," *arXiv:1310.2887*, oct 2013.
- [20] Y. Nesterov, "Efficiency of Coordinate Descent Methods on Huge-Scale Optimization Problems," *SIAM Journal on Optimization*, vol. 22, no. 2, pp. 341–362, jan 2012.
- [21] H. Mansour and O. Yilmaz, "A fast randomized Kaczmarz algorithm for sparse solutions of consistent linear systems," , no. 2, may 2013.
- [22] Y. C. Eldar and D. Needell, "Acceleration of randomized Kaczmarz method via the Johnson-Lindenstrauss Lemma," *Numerical Algorithms*, vol. 58, no. 2, pp. 163–177, 2011.
- [23] X. Gao, O. Edfors, F. Rusek, and F. Tufvesson, "Massive MIMO Performance Evaluation Based on Measured Propagation Data," *IEEE Transactions on Wireless Communications*, vol. 14, no. 7, pp. 3899–3911, jul 2015.
- [24] A. Adhikary, Junyoung Nam, Jae-Young Ahn, and G. Caire, "Joint Spatial Division and Multiplexing—The Large-Scale Array Regime," *IEEE Transactions on Information Theory*, vol. 59, no. 10, pp. 6441–6463, oct 2013.
- [25] E. Bjornson, J. Hoydis, and L. Sanguinetti, "Massive MIMO Has Unlimited Capacity," *IEEE Transactions on Wireless Communications*, vol. 17, no. 1, pp. 574–590, jan 2018.
- [26] A. O. Martinez, E. De Carvalho, and J. O. Nielsen, "Towards very large aperture massive MIMO: A measurement based study," in *2014 IEEE Globecom Workshops (GC Wkshps)*. IEEE, dec 2014, pp. 281–286.
- [27] C. Ingemarsson and O. Gustafsson, "On fixed-point implementation of symmetric matrix inversion," in *2015 European Conference on Circuit Theory and Design (ECCTD)*. IEEE, aug 2015, pp. 1–4.
- [28] C. D. Meyer, *Matrix Analysis and Applied Linear Algebra*. SIAM, 2000.
- [29] W. H. Press, S. A. Teukolsky, W. T. Vetterling, and B. P. Flannery, *Numerical Recipes: The Art of Scientific Computing*, 3rd ed. Cambridge, UK: Cambridge University Press, 2007.
- [30] Y. Censor, P. P. B. Eggermont, and D. Gordon, "Strong underrelaxation in Kaczmarz's method for inconsistent systems," *Numerische Mathematik*, vol. 41, no. 1, pp. 83–92, feb 1983.
- [31] Z. Z. Bai and W. T. Wu, "On partially randomized extended Kaczmarz method for solving large sparse overdetermined inconsistent linear systems," *Linear Algebra and Its Applications*, vol. 578, pp. 225–250, 2019.
- [32] R. Barrett, M. Berry, T. F. Chan, J. Demmel, J. M. Donato, J. Dongarra, V. Eijkhout, R. Pozo, C. Romine, and H. Van der Vorst, *Templates for the Solution of Linear Systems: Building Blocks for Iterative Methods*. Philadelphia, PA: SIAM, 1994.

- [33] Y. Saad, *Iterative Methods for Sparse Linear Systems*, 2nd ed. PWS and SIAM, 2000.
- [34] T. Strohmer and R. Vershynin, "Comments on the Randomized Kaczmarz Method," *Journal of Fourier Analysis and Applications*, vol. 15, no. 4, pp. 437–440, 2009.
- [35] Y. Censor, G. T. Herman, and M. Jiang, "A note on the behavior of the randomized kaczmarz algorithm of Strohmer and Vershynin," *Journal of Fourier Analysis and Applications*, vol. 15, no. 4, pp. 431–436, 2009.
- [36] M. N. Boroujerdi, A. Abbasfar, and M. Ghanbari, "Efficient beam-forming scheme in distributed massive MIMO system," *International Symposium on Turbo Codes and Iterative Information Processing, ISTC*, vol. 2018-Decem, pp. 1–5, 2019.
- [37] G. Kamath, P. Ramanan, and W. Song, "Distributed Randomized Kaczmarz and Applications to Seismic Imaging in Sensor Network," in *2015 International Conference on Distributed Computing in Sensor Systems*, 2015, pp. 169–178.